ISSN 0020-4412, Instruments and Experimental Techniques, 2020, Vol. 63, No. 6, pp. 846–852. © Pleiades Publishing, Ltd., 2020.
Russian Text © The Author(s), 2020, published in Pribory i Tekhnika Eksperimenta, 2020, No. 6, pp. 57–63.

GENERAL EXPERIMENTAL TECHNIQUE

A Supercontinuum Generator with Pumping by Pulses of Chromium–Forsterite-Based Femtosecond Laser in Transparent Condensed Media

I. V. Kryukov[a,b,*], N. Kh. Petrov[a], and M. V. Alfimov[a]

[a] *Photochemistry Center, Russian Academy of Sciences, Federal Research Center "Crystallography and Photonics," Russian Academy of Sciences, Moscow, 119421 Russia*

[b] *Semenov Institute of Chemical Physics, Russian Academy of Sciences, Moscow, 119991 Russia*

**e-mail: igor.v.kryukov@gmail.com*

Received March 17, 2020; revised April 27, 2020; accepted April 29, 2020

Abstract—A facility for generating a supercontinuum in Al_2O_3 and CaF_2 crystals using a femtosecond laser, which is based on a chromium–forsterite (Cr : F) crystal, is described. The supercontinuum spectra under pumping at four wavelengths of 310, 413, 620, and 1240 nm were determined. A continuous spectrum of a supercontinuum from 324 to 1000 nm was obtained in the visible region, thus making it possible to study various samples using the pump–probe system. In the UV spectrum region, the shortest wavelength of a supercontinuum (225 nm) was obtained on the CaF_2 crystal when pumped with pulses at a wavelength of 310 nm.

DOI: 10.1134/S0020441220050309

INTRODUCTION

When focusing a high-intensity femtosecond pulse in a transparent medium, white light from ultraviolet (UV) to infrared (IR), a so-called broadband supercontinuum, is generated. The supercontinuum generation was observed in a variety of transparent materials, including gases, liquids, and solids. Alfano and Shapiro were the first to describe the spectrum-broadening phenomenon in 1970 [1]. They used a high-power picosecond laser with a wavelength of 530 nm and a pulse duration of 5 ps. The continuum generation was studied in BK-7 borosilicate glass, and spectrum broadening from 400 to 700 nm was registered. The first femtosecond supercontinuum was observed in 1983 by Fork et al. [2]. They reported a gigantic spectrum broadening from deep UV (190 nm) to near IR (1600 nm), when focusing high-power femtosecond pulses.

Generating ultrashort pulses with a high repetition rate that are completely tunable in the UV, visible, and near-IR (NIR) bands is still an important task. The continuum generation is used in nonstationary spectroscopy, in the pump–probe method [3, 4]. The continuum generation is widely used in an optical parametric light amplifier [5] and in the system of a noncollinear optical parametric amplifier (NOPA) [6].

The physical picture of the supercontinuum generation in transparent condensed media can be explained within the framework of femtosecond filamentation. The femtosecond filamentation is formed as a result of the interaction between Kerr self-focusing, phase self-modulation, and defocusing laser plasma, which results in the formation of a dynamic structure with an intense core, which can propagate to distances that far exceed the typical diffraction length, while maintaining a narrow beam size without using any external guiding mechanism. The most obvious manifestation of the filament formation is the generation of spatially and temporally coherent ultrawide-band radiation with a low angular divergence, i.e., the supercontinuum generation.

The initial stage of the filament formation is determined by Kerr-type nonlinearity. Let us consider a femtosecond beam that propagates in a medium with a cubic (Kerr) nonlinearity; in this case, the refractive index depends on the intensity as:

$$n = n_0 + n_2 I,$$

where I is the beam intensity, n_0 is the linear refractive index, and n_2 is the nonlinear refractive index related to the optical susceptibility of the material via a third-order (cubic) curve, which is positive in the region of transparency of dielectric media.

The induced change in the refractive index is proportional to the local intensity and is thus higher at the center of the beam and lower at its edges. Therefore, a dielectric medium acts as a lens that focuses the beam. For a cylindrically symmetric Gaussian beam, the

self-focusing threshold is determined by the beam power [7]:

$$P_{cr} = 3.72\lambda^2/(8\pi n_0 n_2),$$

where λ is the laser wavelength; P_{cr} is the critical power of self-focusing, at which the self-focusing effect balances the diffraction propagation of the beam. If the beam power exceeds P_{cr}, a Gaussian beam is then self-focused at the distance [7]

$$Z_{sf} = \frac{0.367k\alpha^2}{\{[(P/P_{cr})^{1/2} - 0.852]^2 - 0.0219\}^{1/2}},$$

where Z_{sf} is the nonlinear focus; α is the beam radius at a level of e^{-1} of the intensity; and $k = 2\pi/\lambda$ is the wave number.

Let us consider the process that is directly responsible for the spectral broadening of a pulse. When an ultrashort Gaussian pulse with a frequency of ω_0 propagates in a dielectric, its intensity as a function of time can be presented in the form

$$I(t) = I_0 \exp(-t^2/t_p^2),$$

where I_0 is the maximum intensity, and t_p is the pulse duration.

Due to the Kerr effect during the pulse propagation, the refractive index at each point of the medium will be a function of the intensity at this point:

$$n(I) = n_0 + n_2 I(t).$$

Let us now consider the case of $n_2 > 0$ that corresponds to self-focusing. At each point of the substance, the intensity first increases and then decreases. This leads to a modulation of the refractive index in time:

$$\frac{dn(I)}{dt} = -\frac{2t}{t_p^2} n_2 I_0 \exp(-t^2/t_p^2).$$

The refractive index that changes with time introduces a nonlinear change into the pulse phase:

$$\varphi_{nl}(t) = -\frac{\omega_0}{c} n_2 I(t) z,$$

where ω_0 is the carrier frequency, and z is the distance that was traveled by a pulse.

The frequency change is then defined by the expression

$$\delta\omega(t) = \frac{d}{dt}\varphi_{nl}(t).$$

The dependence of the instantaneous frequency on time has the form

$$\omega(t) = \omega_0 + \delta\omega(t).$$

Changing the frequency leads to a spectral broadening of a pulse. For a Gaussian laser pulse with a duration t_p, the change in the instantaneous frequency is determined by the expression [8]:

$$\delta\omega(t) = 2\frac{\omega_0}{ct_p^2} n_2 I_0 \exp(-t^2/t_p^2) tz.$$

This effect is called phase modulation; it leads to spectrum broadening due to the induction of a negative shift of the instantaneous frequency at the leading edge of a pulse and a positive shift of the instantaneous frequency at its trailing edge. In other words, the pulse acquires a frequency modulation, which creates spectral components of a red shift at the pulse front and a blue shift at its trailing edge.

However, a beam cannot be focused endlessly: its constant compression in a nonlinear focus is impeded by multiphoton absorption and ionization, thus leading to a loss of the energy and generation of free-electron plasma, which further absorbs and defocuses the beam. The combined influence of these effects limits the intensity to a certain level.

The interaction of femtosecond radiation with the medium is determined by the Kerr nonlinearity and the nonlinearity of laser plasma that occurs upon photoionization in a strong light field of the filament. The nonlinear increment Δn_k of the refractive index n_0, which is caused by the Kerr nonlinearity, is positive and proportional to the field intensity I:

$$\Delta n_k = n_2 I,$$

where n_2 is the cubic nonlinearity factor of the medium.

On the other hand, the increment Δn_p of the refractive index in plasma is negative; in the simplest case, the expression for it has the form

$$\Delta n_p = -\omega_p^2/(2\omega^2),$$

where $\omega_p = (4\pi e^2 N_e/m_e)^{1/2}$ is the plasma frequency; e, m_e, and N_e are, respectively, the electron charge, mass, and concentration; and ω is the optical-field frequency.

In condensed media, laser plasma is generated as a result of electron transitions to the conduction band under the action of laser radiation and avalanche ionization, during which the concentration of electrons in plasma increases exponentially with time.

In a pulse whose peak power exceeds the critical self-focusing power, the intensity increases as the distance to the nonlinear focus decreases. When the power increases to the photoionization threshold, laser plasma is formed, in which defocusing limits a further intensity increase in the nonlinear focus. The dynamic balance of the Kerr self-focusing and plasma defocusing leads to stability of the parameters in an extended femtosecond-pulse filament [9].

This paper describes a supercontinuum generator in transparent condensed media, which is pumped with femtosecond pulses of chromium–forsterite crystal laser. The continuum spectra were measured at four pumping wavelengths: 310, 413, 620, and 1240 nm. Al_2O_3 and CaF_2 crystals were used as condensed media. The supercontinuum generator was developed for the

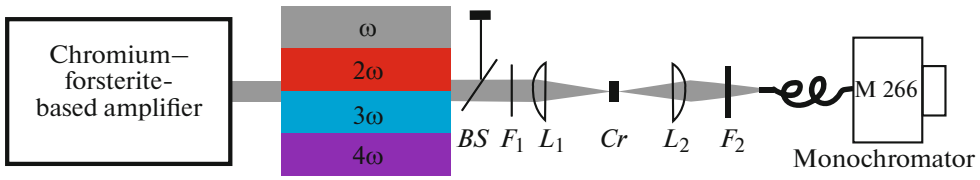

Fig. 1. The supercontinuum generator: (*BS*) beamsplitter; (F_1, F_2) neutral filters with a variable optical density; (L_1, L_2) lenses with focal lengths of 80 (L_1) and 60 mm (L_2); and (*Cr*) CaF_2 or Al_2O_3 crystal.

pump–probe system based on chromium–forsterite [3]. (The authors are not aware of studies on the generation of a supercontinuum in Al_2O_3 and CaF_2 crystals pumped with chromium–forsterite laser radiation.)

A DESCRIPTION OF THE FACILITY

A femtosecond regenerative amplifier on a chromium–forsterite (Cr : F) crystal was used as an amplifier. It consists of a femtosecond-pulse generator, a pumping laser, and a regenerative femtosecond-pulse amplifier. The master laser generates pulses with a duration of 95 fs, an average power of 500 mW, and a repetition frequency of 85 MHz. A pulsed Nd : YAG laser (an LQ629-100 model by Solar LS) is used as the pump source. The pulse energy is 10 J, and the repetition rate is 100 Hz. The center wavelength of an amplified femtosecond pulse is 1240 nm; the half-height width (FWHM) of the spectrum is 17 nm. The pulse energy is 440 μJ; the beam diameter at the amplifier output is 8 mm. The amplifier output radiation is horizontally polarized.

The master laser generates femtosecond pulses with a spectrum FWHM of 22 nm and a duration of 95 fs. After the amplification, the spectrum FWHM decreases to 17 nm. The duration of the amplified pulse that was measured using a correlator is 134 fs.

Let us consider the scheme of the supercontinuum generator (Fig. 1). A block of harmonic generators is installed after the Cr : F-based amplifier: generators of the second, third, and fourth harmonics. All these harmonics are used for pumping in the continuum generator. Various optical mirrors (beam splitters, *BSs*) were used to select the desired pumping wavelength. After the beam splitter (*BS*), a neutral filter (F_1) with a variable optical density is positioned. By moving this filter, one can smoothly change the energy in the pumping radiation beam. An energy of several microjoules is required to generate continuum with femtosecond pulses with a duration of ≈100 fs.

A short-focus lens (L_1) with a focal length of 80 mm focused radiations of the harmonics in an Al_2O_3 or CaF_2 crystal (*Cr*). The pumping intensity in the beam waist reached ~10^{13} W/cm^2. The CaF_2 and Al_2O_3 crystals were 3 mm thick. During the experiment, the CaF_2 crystal was displaced slowly orthogonally to the pumping-beam direction in order to avoid the material degradation. Continuum radiation was collected and focused with a short-focus lens (L_2) with a focal length of 60 mm into a 200-μm-diameter optical fiber. Radiation entered a monochromator through the optical fiber. An M266 monochromator (Solar LS, Minsk) with an entrance slit of 200 μm was used.

Signals were registered in a wide spectral range using a Hamamatsu CMOS linear array (1024 pixels) was used, which operated in the spectral range from 200 to 1000 nm.

Let us consider the optical schemes of harmonic oscillators for the femtosecond regenerative amplifier on (Cr : F). The optical schemes of the second- and third-harmonic oscillators are described in [3].

The fourth-harmonic oscillator consists of a second-harmonic oscillator and the fourth-harmonic oscillator itself (Fig. 2). The second harmonic is generated using an LBO crystal (Cr_1) with a length of 5 mm with an antireflection coating at a wavelength of 1240 nm; the synchronization type is *ooe*. The angle $\varphi = 0°$, the angle $\theta = 87°$. The choice of the LBO crystal is due to the presence of noncritical synchronism at the laser radiation frequency, which allows the use of a long crystal without losses in the spectrum and, accordingly, without a significant increase in the pulse duration.

Radiation from the amplifier was focused in the crystal Cr_1 by the long-focus lens L_1 with a focal length of 50 cm (see Fig. 2). The nonlinear crystal was located in front of the focal point (out of focus). The coefficient of conversion to the second harmonic (equal to 50%) was achieved at an intensity of ~50 GW/cm^2 for a main wavelength of 1240 nm. The maximum power of the second harmonic was 220 mW, which corresponded to a pulse energy of 220 μJ.

A higher conversion coefficient, 60% or more, can also be obtained; however, due to self-focusing, the transverse intensity distribution of the second harmonic is greatly worsened in this case. Radiation at the main frequency and the frequency of the second harmonic was collected after the crystal by the lens L_2 with a focal length of 30 cm. The beamsplitter (BS_1) reflected radiation of the second harmonic and transmitted radiation of the main harmonic, which was blocked by a protective shield.

After passing through the splitters BS_1 and BS_2, radiation of the second harmonic was focused in a

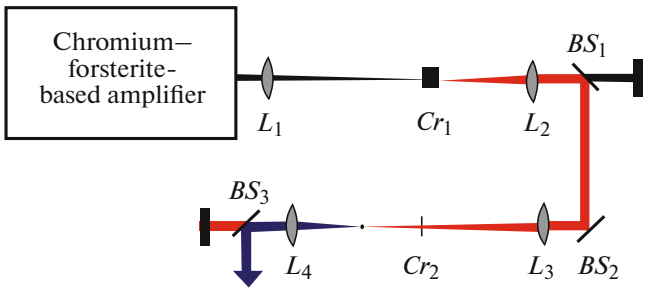

Fig. 2. The optical scheme of the fourth-harmonic generation: (L_1–L_4) lenses with focal lengths of 50 (L_1), 30 (L_2), 25 (L_3), and 20 cm (L_4); $(Cr)_1$ 5-mm-long LBO crystal; (BS_1–BS_3) beamsplitters; and (Cr_2) 0.5-mm-long BBO crystal.

BBO crystal (Cr_2) with a length of 0.5 mm using the lens L_3 with a focal length of 25 cm for generating the fourth harmonic. The nonlinear crystal Cr_2 is placed in front of the focal point. The synchronism type is *ooe*, $\theta = 28°$, and $\varphi = 90°$. After the crystal Cr_2, radiations of the second and fourth harmonics were collected by the lens L_4 with a focal length of 20 cm. A beamsplitter BS_3 reflected radiation of the fourth harmonic and transmitted radiation of the second harmonic, which was blocked by the protective shield. The fourth-harmonic radiation is polarized horizontally; its wavelength is 310 nm.

The maximum power of the fourth harmonic is 40 mW, which corresponds to a pulse energy of 40 μJ.

A SUPERCONTINUUM GENERATOR WITH PUMPING AT A WAVELENGTH OF 1240 nm

Figures 3a and 3b show the supercontinuum spectra in CaF_2 and Al_2O_3 crystals, respectively, that are pumped at a wavelength of 1240 nm.

According to this figure, the spectrum of a supercontinuum in the anti-Stokes region is essentially nonmonotonic. A peak shifted to the blue spectrum region occurs in the visible portion of the spectrum. The center wavelengths of the anti-Stokes peaks for the Al_2O_3 and CaF_2 crystals were 580 and 600 nm, respectively. In the Saliminia experiments [10], the boundary of the short-wave region of the supercontinuum spectrum was 400 nm. In our experiments, the boundary of the short-wave region of the supercontinuum spectrum for the CaF_2 crystal was 324 nm. This is due to the fact that the width of the forbidden zone of the CaF_2 crystal (10.2 eV [11]) is larger than that of fused quartz (7.5 eV [11]), while the anti-Stokes broadening of the supercontinuum spectrum is proportional to the ratio of the forbidden-zone width to the radiation photon energy $h\omega$ [12].

The supercontinuum spectra that are shown in Fig. 3 are very interesting for practical application. The supercontinuum spectrum for the CaF_2 crystal ranges from 324 to 1000 nm. This option is very convenient for operating in the pump–probe system, since it makes it possible to study samples in a wide spectral range.

In our case, a supercontinuum generator that uses a Cr : F-based femtosecond amplifier as the pump source has an advantage over a supercontinuum generator pumped with a titanium-sapphire-based femtosecond amplifier, which is most frequently used. The center wavelength of a titanium–sapphire laser is $\lambda = 800$ nm. When an Al_2O_3 crystal is pumped by a titanium laser, the obtained supercontinuum spectrum ranges from 400 to 1600 nm; however, there is a pumping peak with a width of 770–830 nm in a region of 800 nm. Investigating samples in this spectrum region requires that the pumping peak be cut off by specially selected filters, which is a difficult problem. When chromium–forsterite is used, as follows from Fig. 3a, a wide continuous spectrum of a supercontinuum from 324 to 1000 nm is obtained without the presence of a pump-

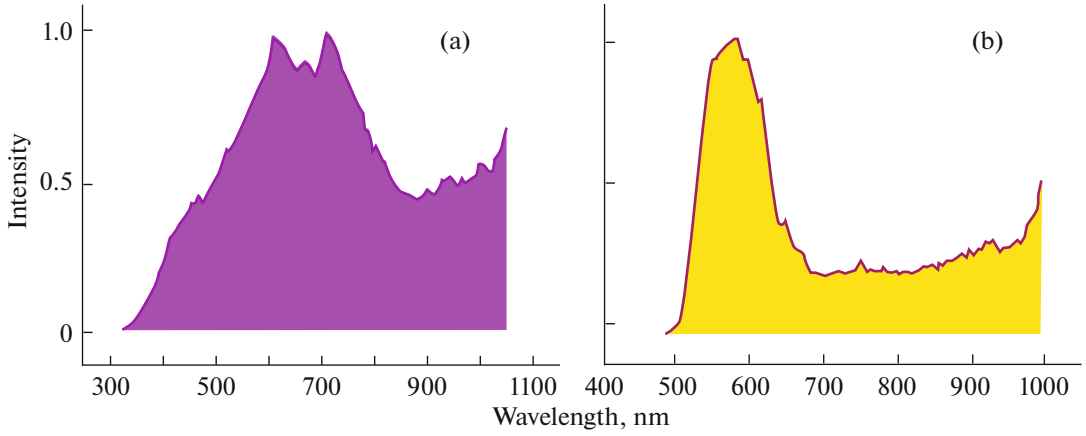

Fig. 3. The spectra of a supercontinuum generated in (a) CaF_2 and (b) Al_2O_3 crystals with pumping at a wavelength of 1240 nm.

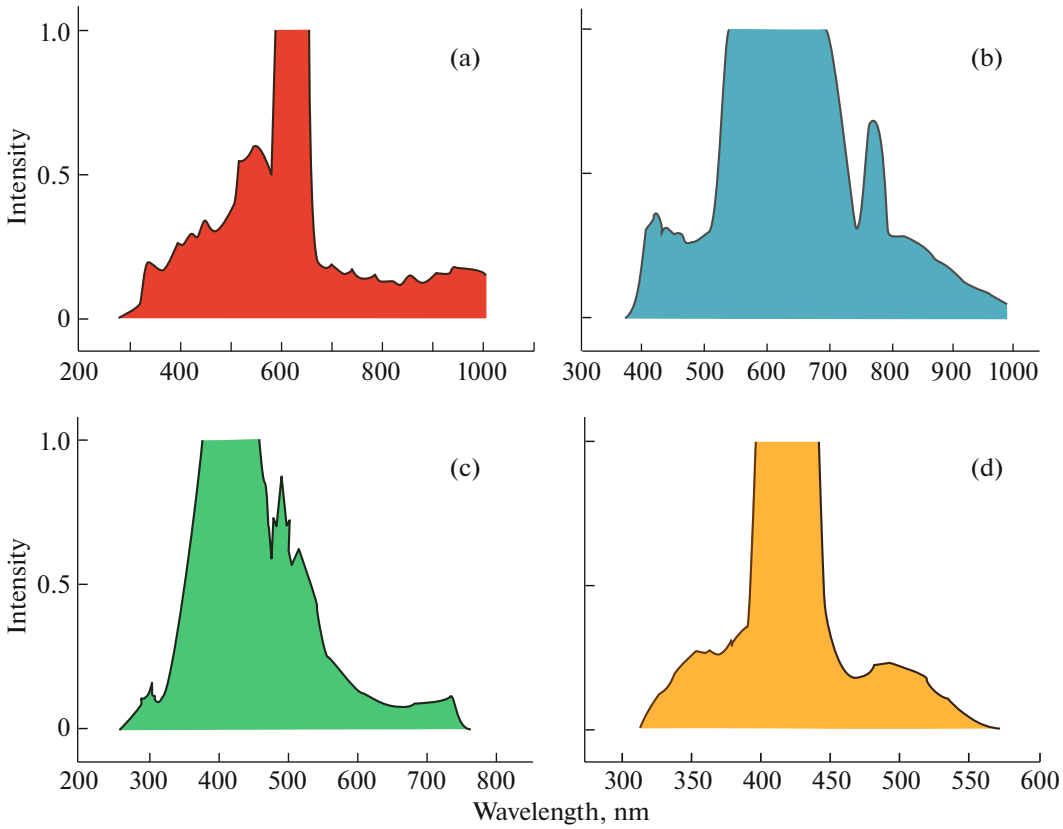

Fig. 4. The spectra of a supercontinuum generated in (a, c) CaF_2 and (b, d) Al_2O_3 crystals with pumping at wavelengths of (a, b) 620 and (c, d) 413 nm.

ing peak, thus allowing this spectrum to be used without additional filters.

A SUPERCONTINUUM GENERATOR PUMPED AT WAVELENGTHS OF 620 AND 413 nm

The most popular crystal for continuum generation is an Al_2O_3 (sapphire) crystal. This crystal is often used to generate a supercontinuum with titanium–sapphire-based femtosecond lasers, because it is highly nonlinear and has a high optical breakdown threshold. This ensures the high quality of the seed signal, thus contributing to the development of modern femtosecond optical parametric amplifiers [13, 14]. The famous Light Conversion Company uses an Al_2O_3 crystal in its TOPAS optical parametric amplifier in the continuum generator for good reasons.

Figures 4a and 4b show the supercontinuum spectra obtained for the CaF_2 and Al_2O_3 crystals, respectively, with pumping at a wavelength of 620 nm. The widest supercontinuum spectrum was obtained for the CaF_2 crystal: from 282 to 1000 nm; for Al_2O_3, the width of the supercontinuum spectrum covers a wavelength range of 380–1000 nm.

Figures 4c and 4d show the supercontinuum spectra that were obtained for the CaF_2 and Al_2O_3 crystals under pumping at a wavelength of 413 nm, respectively. The supercontinuum spectra for the CaF_2 and Al_2O_3 crystals cover wavelength ranges of 248–745 and 310–565 nm, respectively.

From the practical point of view, when using supercontinuum generators with pumping at wavelengths of 620 and 413 nm in pump–probe systems, it is necessary to use specially selected optical filters that cut off the spectral region where pumping occurs.

A SUPERCONTINUUM GENERATOR WITH PUMPING AT A WAVELENGTH OF 310 nm

For femtosecond spectroscopy of the nonstationary absorption in the visible spectrum region, a white-light (continuum) source is required to probe the dynamics of absorption changes in a wide spectral range. The ability to generate a continuum in the near UV region is of greatest interest, since a large number of organic compounds absorb in this spectrum region.

Alkali metal fluorides are promising materials for generating a supercontinuum. A special place among them is occupied by LiF crystals, which have the wid-

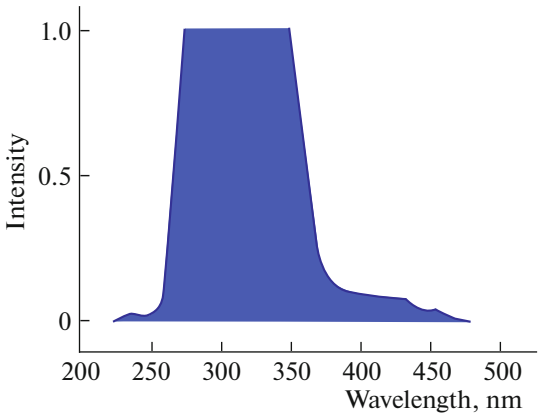

Fig. 5. The spectrum of a supercontinuum generated in the CaF_2 crystal with pumping at a wavelength of 310 nm.

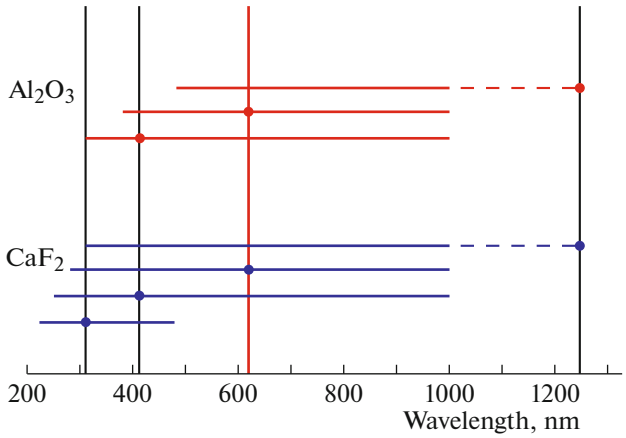

Fig. 6. Supercontinuum spectra.

est transparency region and the widest forbidden zone (11.8 eV) [11]. The most significant broadening of the supercontinuum spectra to the UV region is observed in this material during femtosecond filamentation. A special feature of a LiF crystal is that color centers are formed in it under the action of high-power laser radiation, causing both a change in the refractive index in the region from the UV to the medium IR range and the appearance of absorption bands.

The influence of color centers on the spectral characteristics of a supercontinuum was studied in [15]. It was shown experimentally that during the long-term irradiation of a LiF crystal and the appearance of color centers, an absorption band with a center at a wavelength of 250 nm arises, thus reducing the supercontinuum-spectrum width.

LiF and CaF_2 crystals are the record holders for generating a supercontinuum in the UV spectrum region; the shortest wavelengths were obtained with them.

In [15], the widths of the supercontinuum spectra generated in LiF and CaF_2 crystals with pumping at a wavelength of 775 nm were compared. In the UV spectrum region in the CaF_2 crystal, the shortest supercontinuum wavelength was 287 nm, while in the LiF crystal, it was 270 nm, which is 17 nm less than in CaF_2.

We studied the generation of a supercontinuum in the CaF_2 crystal with pumping at a wavelength of 310 nm; the obtained supercontinuum spectrum ranges from 225 to 480 nm (Fig. 5). The shortest wavelength of the continuum spectrum was 225 nm.

Figure 6 shows the combined experimental results of broadening the supercontinuum spectra for the CaF_2 and Al_2O_3 crystals. The highest value of anti-Stokes broadening was achieved at a pumping wavelength of 1240 nm with the CaF_2 crystal. The minimum wavelength of the supercontinuum spectrum was 324 nm. The shortest wavelength of the supercontinuum spectrum (225 nm) was achieved at a pumping wavelength of 310 nm.

CONCLUSIONS

A supercontinuum generator with pumping by femtosecond pulses from a chromium–forsterite-based laser was created. The generation of a supercontinuum in various condensed media was studied at four pumping wavelengths: 310, 413, 620, and 1240 nm, in order to apply the obtained data in a pump–probe system. The generation of a supercontinuum in a CaF_2 crystal with pumping at a wavelength of 1240 nm is promising. The width of the generated supercontinuum spectrum was 324–1000 nm (with the absence of pumping), thus making it possible to study samples in a wide wavelength range. Measurements in the UV spectrum region showed that with a chromium–forsterite-based amplifier it is possible to generate a supercontinuum in the short-wavelength part of the UV spectrum region. The shortest wavelength of 225 nm was obtained in the CaF_2 crystal when pumped with pulses at a wavelength of 310 nm.

FUNDING

This study was supported by the Ministry of Science and Higher Education within the framework of the State Job of the Crystallography and Photonics Federal Research Center of the Russian Academy of Sciences.

REFERENCES

1. Alfano, R. and Shapiro, L., *Phys. Rev. Lett.,* 1970, vol. 24, p. 584. https://doi.org/10.1103/PhysRevLett.24.584
2. Fork, R., Shank, C., Hirlimann, C., Yen, R., and Tomlinson, W., *Opt. Lett.,* 1983, vol. 8, p. 1. https://doi.org/10.1364/OL.8.000001
3. Kryukov, I.V., Petrov, N.Kh., Ivanov, A.A., and Alfimov, M.V., *Instrum. Exp. Tech.,* 2019, vol. 62, no. 4, p. 548. https://doi.org/10.1134/S0020441219040079

4. Kovalenko, S.A., Ernsting, N.P., and Ruthmann, J., *Chem. Phys. Lett.,* 1996, vol. 258, p. 445. https://doi.org/10.1016/0009-2614(96)00647-1
5. Cerullo, G. and De Silvestria, S., *Rev. Sci. Instrum.,* 2003, vol. 74, p. 1. https://doi.org/10.1063/1.1523642
6. Bradler, M. and Riedle, E., *Opt. Lett.,* 2014, vol. 39, p. 2588. https://doi.org/10.1364/OL.39.002588
7. Marburger, J.H., *Prog. Quantum Electron.,* 1975, vol. 4, p. 35. https://doi.org/10.1016/0079-6727(75)90003-8
8. Dubietis, A., Tamošauskas, G., Šuminas, R., Jukna, V., and Couairon, A., *Lith. J. Phys.,* 2017, vol. 57, p. 113. https://doi.org/10.3952/physics.v57i3.3541
9. Kandidov, V.P., Shlenov, S.A., and Kosareva, O.G., *Kvantovaya Elektron.,* 2009, vol. 39, no. 3, p. 205.
10. Saliminia, A., Chin, S.L., and Vallée, R., *Opt. Express,* 2005, vol. 13, p. 5731.
11. Brodeur, A. and Chin, S.L., *J. Opt. Soc. Am. B,* 1999, vol. 16, p. 637. https://doi.org/10.1364/JOSAB.16.000637
12. Nagura, C., Suda, A., Kawano, H., Obara, M., and Midorikawa, K., *Appl. Opt.,* 2002, vol. 41, p. 3735. https://doi.org/10.1364/AO.41.003735
13. Brida, D., Manzoni, C., Cirmi, G., Marangoni, M., Bonora, S., Villoresi, P., De Silvestri, S., and Cerullo, G., *J. Opt.,* 2010, vol. 12, p. 1. https://doi.org/10.1364/OL.33.000741
14. Manzoni, C. and Cerullo, G., *J. Opt.,* 2016, vol. 18, p. 1. https://doi.org/10.1088/2040-8978/18/10/103501
15. Kohl-Landgraf, J., Nimsch, J., and Wachtveitl, J., *Opt. Express,* 2013, vol. 21, p. 17060. https://doi.org/10.1364/OE.21.017060

Translated by A. Seferov